Mahmoud EY *et al.* (2025)
Notulae Botanicae Horti Agrobotanici Cluj-Napoca
Volume 53, Issue 4, Article number 14717
DOI:10.15835/nbha53414717
Research Article

Reduction of peanut pod rots and aflatoxin contamination using selected micronutrient nanoparticles

Emad Y. MAHMOUD[1], Zeinab N. HUSSIEN[1], Mohamed I. AHMED[1], Ahlam E. ABDELAAL[1], Wael F. SHEHATA[2*], Samiyah S. AL-ZAHRANI[3], Mohamed A. ABOU-ZEID[1*]

[1]*Plant Pathology Research Institute, Agricultural Research Center, Giza, 12619, Egypt; Emad.qotp@arc.sci.eg; zne.flower@gmail.com; mim_ahmed1912@yahoo.com; ahlamamer2018@gmail.com; m.abouzeid@arc.sci.eg (*corresponding author)*
[2]*King Faisal University, College of Agriculture and Food Sciences, Department of Agricultural Biotechnology, Al-Ahsa, 31982, Saudi Arabia; wshehata@kfu.edu.sa (*corresponding author)*
[3]*Al-Baha University, Faculty of Science, Department of Biology, Al Baha, 65779, Saudi Arabia; sshassan@bu.edu.sa*

Abstract

Climate-induced biological changes have altered host–pathogen interactions, highlighting the urgent need to strengthen plant defense mechanisms using environmentally safe alternatives to conventional fungicides that often pose ecological risks. This study evaluated the efficacy of micronutrient nanoparticles-iron oxide (Fe_3O_4), manganese oxide (MnO), and zinc oxide (ZnO)-at concentrations of 0, 25, 50, and 100 mg L^{-1} in mitigating peanut (*Arachis hypogaea* L.) pod rot and reducing contamination by aflatoxigenic fungi (*Aspergillus flavus* and *A. parasiticus*). Greenhouse and field trials were conducted during the 2022 and 2023 growing seasons to assess their effects on disease incidence, fungal frequency, aflatoxin levels, yield performance, and associated biochemical responses. All nanoparticle treatments significantly reduced pod-rot incidence and aflatoxigenic fungal contamination, with concomitant improvements in yield relative to the untreated control Fe_3O_4 nanoparticles at 100 mg L^{-1} exhibited the most excellent efficacy, achieving marked reductions in disease severity and aflatoxin accumulation, while enhancing the activity of antioxidant enzymes (peroxidase, polyphenol oxidase, and catalase) and increasing phenolic compounds, sugars, free amino acids, and protein content. MnO nanoparticles also showed notable but comparatively lower effects, whereas high concentrations of ZnO nanoparticles were associated with increased fungal infection and aflatoxin levels. The findings highlight the potential of micronutrient nanoparticles, particularly Fe_3O_4, as eco-friendly resistance inducers that enhance both biochemical and physiological defenses in peanut plants under biotic stress, provided their concentrations are carefully optimized.

Keywords: aflatoxin contamination; antifungal activity; micronutrient nanoparticles; peanut pod rots; plant pathology; sustainable agriculture

Received: 14 Aug 2025. Received in revised form: 19 Oct 2025. Accepted: 09 Nov 2025. Published online: 10 Dec 2025.
From Volume 49, Issue 1, 2021, Notulae Botanicae Horti Agrobotanici Cluj-Napoca journal uses article numbers in place of the traditional method of continuous pagination through the volume. The journal will continue to appear quarterly, as before, with four annual numbers.

Introduction

Peanut (*Arachis hypogaea* L.) is the fourth most widely cultivated oilseed crop worldwide, primarily grown for its grains and oil. It serves as a vital source of protein and vegetable oil, with global cultivation spanning over 30.65 million hectares across more than 100 countries, yielding over 51 million tons annually (USDA, 2024). In Egypt, peanut is among the most important cash crops for both local consumption and export, occupying approximately 61,442 hectares with a production of 218,835 tons (FAO STAT, 2024).

Despite its economic and nutritional significance, peanut production faces significant biotic challenges, most notably pod rot diseases and aflatoxin contamination, both of which substantially affect yield and quality. Pod rot is one of the most destructive diseases attacking peanut plants, leading to significant quantitative and qualitative yield losses that may reach 15–50%, and in severe cases, complete crop failure (He *et al.,* 2022; Liu *et al*., 2024; Mahmoud *et al.,* 2024). The disease is associated with a complex of soil-borne pathogens, including *Fusarium moniliforme*, *Macrophomina phaseolina*, *Rhizoctonia solani*, *Sclerotium rolfsii*, and *Pythium* spp. (Liu *et al.,* 2024; Mahmoud *et al.,* 2015, 2024). Aflatoxin contamination remains a significant concern in groundnut production, necessitating the integration of nanotechnology-based micronutrient formulations as eco-safe control alternatives.

Simultaneously, aflatoxin contamination, especially under preharvest conditions, represents a serious health and trade concern for peanut producers worldwide. Although contamination may occur before or after harvest, the preharvest phase is considered the most critical (Mahmoud *et al.,* 2015; Bediako *et al*., 2019*;* Kankam *et al*., 2021). In Egypt, *Aspergillus flavus* Link and *A. parasiticus* Speare are the predominant aflatoxigenic fungi infecting peanuts before harvest (Mahmoud *et al.,* 2015, 2024). Ample evidence has demonstrated that these fungi are capable of invading peanut pods and producing aflatoxins while still in the field (Mahmoud *et al.,* 2015; Bediako *et al.,* 2019; Kankam *et al*., 2021).

Efforts to manage pod rot and pre-harvest aflatoxin contamination remain challenging due to the wide host range of the pathogens involved and the absence of commercially resistant cultivars (Mahmoud *et al.,* 2015; He *et al.,* 2022; Liu *et al.,* 2024). These difficulties highlight the urgent need for practical, sustainable, and integrated disease management strategies, including the potential use of micronutrients and nanotechnology-based solutions.

In this context, the application of micronutrients is widely recognized as a fundamental approach to maintaining plant health, enhancing disease resistance, and alleviating physiological disorders. Several studies (Mahmoud *et al.,* 2009; Fouda, 2017; Tsewang *et al.,* 2024) have highlighted the critical roles of micronutrients in regulating numerous metabolic and physiological processes directly linked to plant defense mechanisms. In this respect, micronutrients such as zinc, iron, manganese, and copper are essential for enzymatic activation, chlorophyll biosynthesis, and the production of secondary metabolites, including phenolic, flavonoids, and phytoalexins, which serve as defensive compounds against various pathogens. Specifically, zinc contributes to the activity of antioxidant enzymes and stabilizes cell membranes under biotic stress. Iron is involved in redox reactions and energy transfer, both of which are crucial for photosynthesis and overall plant vigor. Manganese acts as a cofactor for key enzymes such as peroxidase and catalase, which help scavenge reactive oxygen species and enhance the plant's tolerance to oxidative stress (Mahmoud *et al.,* 2009; Sirelkhatim *et al.,* 2015; Singh *et al.,* 2016; Zafar *et al.,* 2016; Fouda, 2017; García-López *et al.,* 2018; Salvia *et al.,* 2023; Abdelbaset *et al.*, 2024; Tsewang *et al.,* 2024). Moreover, sufficient availability of micronutrients has been shown to reduce disease severity by strengthening structural and biochemical barriers within plant tissues, thereby limiting pathogen invasion and proliferation. Tsewang *et al.* (2024) demonstrated that micronutrient supplementation not only improved resistance to fungal and bacterial pathogens but also mitigated nutrient deficiency symptoms such as chlorosis, stunted growth, and poor reproductive performance.

In recent years, the development and utilization of micronutrient-based nanoparticles (NPs) have emerged as an innovative and promising approach in sustainable agriculture. Nanoparticles such as ZnO, Fe_3O_4, and MnO

offer several advantages over conventional formulations due to their ultra-small size, high surface area, enhanced reactivity, and superior bioavailability. These physicochemical properties enable more efficient absorption and translocation within plant tissues, resulting in accelerated physiological responses and more effective mitigation of biotic and abiotic stresses (Singh *et al*., 2016; Zafar *et al*., 2016; Omar *et al*., 2012; Pan and Xing, 2012; An *et al*., 2022; Vijayreddy *et al*., 2023; Atwa *et al*., 2025).

The present study aimed to evaluate the potential of selected micronutrient nanoparticles in inducing resistance in peanut plants against pod rot disease and aflatoxigenic fungi, and in reducing aflatoxin accumulation in seeds. It was hypothesized that Fe_3O_4 nanoparticles, at optimized concentrations, would exhibit superior efficacy compared to MnO and ZnO nanoparticles by mitigating disease severity and aflatoxin contamination while enhancing defense-related biochemical activities.

Materials and Methods

Isolation of causal organisms

The authors previously isolated the fungal isolates used throughout this study from diseased peanut pods, and their pathogenic capabilities were also confirmed (Zeinab-Hussien and Gomaa, 2020).

Preparation of fungal inoculum

(A): Inocula of *Fusarium moniliforme*, *Sclerotium rolfsii, Macrophomina phaseolina*, and *Rhizoctonia solani* were prepared using sorghum-coarse sand-water (2:1:2 v/v) medium. Inoculum preparation and inoculation were performed exactly as described by Filonow *et al*. (1988).

(B): Inocula of aflatoxigenic fungi, i.e., *Aspergillus flavus* and *A. parasiticus,* were prepared, as described by Youssef *et al*. (1999).

Soil infestation with pod rot fungi and aflatoxigenic fungi

Two different methods for soil infestation with the pathogens tested were used throughout this study:

(A): Mixture *of F. moniliforme, M. phaseolina, R. solani, and S. rolfsii for* studying pod rots complex diseases, the inocula were mixed thoroughly with the soil surface of each pot, at the rate of 2% w/w, and were covered with a thin layer of sterilized soil. Infested pots were irrigated and kept for 7 days until sowing.

(B): Each Kg of soil was infested with 10 ml conidial suspension (4 × 10^4 spores/ml) of separately and mixed isolates of Aspergillus flavus and A. parasiticus, 30 days after sowing, to study the effect of aflatoxigenic fungi and aflatoxin contamination.

Source and characterization of nanoparticles (Fe_3O_4NPs, MnO NPs, and ZnONPs)

The nanoparticles used in this study, iron oxide (Fe_3O_4 NPs), manganese oxide (MnO NPs), and zinc oxide (ZnO NPs), were obtained from the Nanotechnology and Advanced Nano Materials Laboratory (NANML), Plant Pathology Research Institute, Agricultural Research Center (ARC), Egypt. A comprehensive physicochemical characterization of the nanoparticles was carried out at the same facility. In this respect, High-Resolution Transmission Electron Microscopy (HR-TEM; Tecnai G2, FEI, Netherlands) was employed to examine particle morphology. Dynamic Light Scattering (DLS) analysis was performed to determine particle size distribution, while X-ray Diffraction (XRD) analysis was used to investigate the crystallographic structure of the nanoparticles.

Preparation of nanoparticle stock suspensions and working solutions

Dry powders of Fe_3O_4, MnO, and ZnO nanoparticles were dispersed in sterile deionized water to prepare 1 g L^{-1} (1000 mg L^{-1}) stock suspensions. For each stock, [mg] of powder was weighed and brought to

[mL] in a Class-A volumetric flask, then pre-mixed by vortexing for 60 s. Suspensions were sonicated using a [bath/probe sonicator, model, manufacturer] for [total time] with [settings: e.g., 40 kHz bath; or probe at % amplitude, 2 s on/1 s off pulse], with the flask kept in an ice bath to limit heating (≤ 25 °C). Immediately before use, stocks were re-sonicated for [2-3] min. Working solutions of 25, 50, and 100 mg L^{-1} were prepared by volumetric dilution of the stock with sterile deionized water, mixed by vortexing (30 s) and brief sonication (1-2 min). No dispersants were added. To confirm adequate dispersion, the hydrodynamic diameter and PDI of each NP in working suspensions were verified by DLS prior to application. All suspensions were prepared fresh on the day of spraying (Atwa *et al*., 2025).

Foliar treatments

The effects of three micronutrients ,Fe_3O_4 NPs, MnO NPs, and ZnO NPs, applied at concentrations of 25, 50, and 100 mg L^{-2}, were evaluated on the severity of pod rot diseases, occurrence of aflatoxigenic fungi, and seed aflatoxin contamination. Each micronutrient was applied as a foliar spray at 20 and 40 days from sowing. Additionally, the fungicide Baler (Azoxystrobin and Difenoconazole) was applied as a foliar spray at a rate of 300 mL/feddan, three times at 15-day intervals, starting 30 days after transplanting. While fungicide Balear SC 50% (Chlorothalonil PHI 10 days) was applied as a soil drench after 50 days from sowing at the rate of 7.5 liters/fedd.

Disease assessment

(A) At harvest, the percentage of pod rot was recorded. Four categories for apparent symptoms of pod rots beside the healthy pods were adopted according to Satour *et al. (1978) a) Rhizoctonia* rot, pods with dry brown lesions, b) *Fusarium rot,* pods with pink discoloration, and c) complex rot pod with general breakdown resulting from many fungi.

(B) Aflatoxigenic fungi, which are associated with the four categories, were isolated after harvesting according to Garren and Porter (1970). Two seed fruits were shelled, and 1cm^2 pieces of shell and seed were surface-disinfested for three minutes in 1% sodium hypochlorite and plated on potato dextrose agar (PDA) medium (4 plates in 4 replicates, 5 seeds or shell pieces per dish). Plates were examined after 7 days of incubation at 27°C for fungal propagules. Identification of the isolates was carried out based on taxonomic criteria for these fungi as described by Maren and Johan (1988).

Determination of aflatoxin

Aflatoxins were extracted and determined according to A.O.A.C. (2000). The concentrations were estimated by external calibration using a single level height near the desired height of the sample under test.

The following equation was used for calculation:

$$Cs = \frac{V}{Va} \times \frac{Vf}{W} \times \frac{h_{sam}}{h_{st}} \times Y$$

V**=** Extraction volume (ml)
Va= Aliquot taken from the extraction volume (ml)
Vf= Final dilution volume (ml)
hsam= The height of the sample peak
hst= The height of the standard peak
Y = Standard concentration (ng/ml).
W = Weight of sample taken for test (g).

Greenhouse experiment

Ten seeds were planted in 50 cm diameter-disinfested plastic pots, which contained sterile sandy clay soil 2:1 previously autoclaved for 2 hours. Five replications were used for each treatment and allocated in the greenhouse following a complete randomized block design.

Disinfested seeds of Giza 6 peanut cultivars were sown in potted soil containing inoculum, about 100g (2% w/w) of a manually mixed inoculum of *R. solani, S. rolfsii, F. moniliforme,* and *M. phaseolina,* to determine the effect of microelements on pod rot diseases or artificial inoculation by *Aspergillus flavus* and *A. parasiticus* separately. Their mixtures were used to determine the effect of microelements on the occurrence of aflatoxigenic fungi and the content of aflatoxin contamination.

Field experiment

Field experiments were carried out during the 2022 and 2023 seasons, in naturally infested field soil, at a private farm in Nobaria, El Beheira Governorate. The soil type was sandy loam (65% sand, 15% silt, 20% clay; pH 7.8 and EC 8.21). To assess the effect of micronutrients as foliar treatments on the incidence of pod rot and invasion by aflatoxigenic fungi under field conditions. Peanut seeds, cvGiza 6, were used for sowing throughout this study. Seeds were sown in the first week of May with 10 cm spacing between plants. The experimental unit area was 10.5 m2 (1/400 fed.). Each plot includes six rows, 3.5m in length and 50 cm in width. The experiment was arranged in a completely randomized block design with four replicates. Cultural practices such as fertilization, irrigation, and pest control were carried out as usual. Plants in individual plots were dug and inverted based on an optimum maturity index. Pods were threshed, air-dried for three days, weighed, and then examined for pod rot incidence.

Meanwhile, the percentage of yield loss was calculated using the following formula:

$$Increase\ of\ yield\ \% = \left(\frac{Yield\ of\ treatment\ - Yield\ of\ control}{Yield\ of\ control}\right) \times\ 100$$

The frequency of invasion by aflatoxigenic fungi was recorded in each pod rot type, and the content of aflatoxins was determined in apparently healthy pods, 15 days after harvest, as previously described.

Biochemical changes associated with microelements treatments

Primordial pods (15 days old) samples were taken and extracted according to Goldschmidt *et al.* (1968), then activities of the oxidative enzymes *i.e.,* peroxidase (PO); polyphenol oxidase (PPO) and catalase (CAT) were determined as described by Walter and Purcell (1980), Thimmaiah (1999), and Mueller *et al.* (1997) and assayed using a spectrophotometer at 425, 495 and 240 nm. The reaction substrate of each oxidative enzyme was pyrogallol, catechol, and H_2O_2 for determining the activity of peroxidase, polyphenol oxidase, and catalase, respectively. Other samples were extracted in Soxhlet units using 75% ethanol for 10-12 h, then used to determine phenolic compounds, sugar content, total free amino acids, and percentage of crude protein as described by Thomas and Dutcher (1924), Snell and Snell (1953), Moore and Stein (1954), and A.O.A.C. (1998), respectively. The phenols, sugars, and total free amino acids contents were also calculated as milligrams equivalent of catechol, glucose, and arginine per gram fresh weight of peanut primordial pods (15 days old), respectively.

Statistical analysis

Statistical analysis of variance (ANOVA) was performed using CoStat version 6.4 (CoHort Software, Monterey, CA, USA). Prior to analysis, data were checked for normality (Shapiro–Wilk test) and homogeneity of variances (Levene's test) to ensure compliance with ANOVA assumptions. Mean separation was conducted using Duncan's Multiple Range Test (DMRT) at a significance level of $P < 0.05$, assuming independent and

normally distributed residuals. All subsequent data processing, regression modeling, and figure generation were carried out in Python 3.9 within Jupyter Notebook 6.4, employing pandas and statsmodels for data manipulation and analysis, and matplotlib for high-quality visualizations (Reback, 2021). Principal Component Analysis (PCA) was applied to the standardized biochemical variables to elucidate treatment-driven patterns; PCA computation and score-loading extraction were performed using the PCA module of scikit-learn (Pedregosa *et al*., 2011; Atia *et al*., 2021) and visualized with matplotlib.

Results

Characterization of nanoparticles (Fe_3O_4NPsMnO NPs, and ZnO NPs)

The physicochemical properties of the synthesized Fe_3O_4, MnO, and ZnO nanoparticles (NPs) were characterized using various analytical techniques, as summarized in Table 1 and illustrated in Figure 1. High-Resolution Transmission Electron Microscopy (HR-TEM) was employed to investigate the particle size and morphology of the nanoparticles. The HR-TEM images (Figures 1A, B, and C) revealed that all three types of nanoparticles exhibited a nearly spherical shape, with average particle sizes of 55 ± 19 nm for Fe_3O_4 NPs, 15 ± 22 nm for MnO NPs and 85 ± 12 nm for ZnO NPs.

The crystalline structure of the nanoparticles was further confirmed by X-ray diffraction (XRD) analysis. The XRD pattern of Fe_3O_4 NPs (Figure 1A) exhibited prominent peaks at 2θ values of approximately 30.1°, 35.5°, 43.1°, 53.4°, 57.0°, and 62.6°, corresponding to the (220), (311), (400), (422), (511), and (440) planes, respectively. These peaks are in good agreement with the standard magnetite phase (Fe_3O_4) according to JCPDS card No. 19-0629, indicating a cubic spinel structure. The sharp and intense peaks confirm the high crystallinity of the sample, while moderate peak broadening suggests the formation of nanocrystalline domains. Similarly, the XRD pattern of MnO NPs (Figure 1B) showed distinct diffraction peaks in the 2θ range of 20°-60°, with significant peaks observed at approximately 28.8°, 32.3°, and 36.0°, corresponding to the (111), (200), and (220) crystal planes of the cubic MnO phase. These results confirm the crystalline nature of the nanoparticles. While, the XRD pattern of ZnO NPs (Figure 1C) exhibited sharp peaks at 2 values of 31.7°, 34.4°, 36.2°, 47.5°, 56.6°, 62.8°, 67.9°, and 68.9°, which correspond to the (100), (002), (101), (102), (110), (103), (112), and (201) planes, respectively. These reflections match the hexagonal wurtzite structure of ZnO, in accordance with JCPDS card No. 36-1451. The absence of secondary peaks confirms the phase purity of the ZnO NPs, while the sharp and well-defined peaks indicate high crystallinity and nanostructured nature.

Greenhouse experiments

Effect of some microelement nanoparticles on peanut pod rots diseases

The data presented in Table 2 highlight the significant impact of micronutrient nanoparticles on reducing peanut pod rot incidence under greenhouse conditions. All tested nanoparticles (Fe_3O_4 NPs, MnO NPs, and ZnO NPs) demonstrated a concentration-dependent suppression of disease symptoms, with higher concentrations generally exhibiting greater efficacy.

Table 1. General and physicochemical properties of nano-materials

Nano-materials	Properties			
	Appearance (color)	Appearance (form)	Shape	Size
Fe_3O_4 NPs	Dark brown	solution	Spherical	55± 19 nm
MnO NPs	Pale white	solution	Spherical	85 ± 12 nm
ZnO NPs	White to yellow	solution	Spherical	85± 12nm

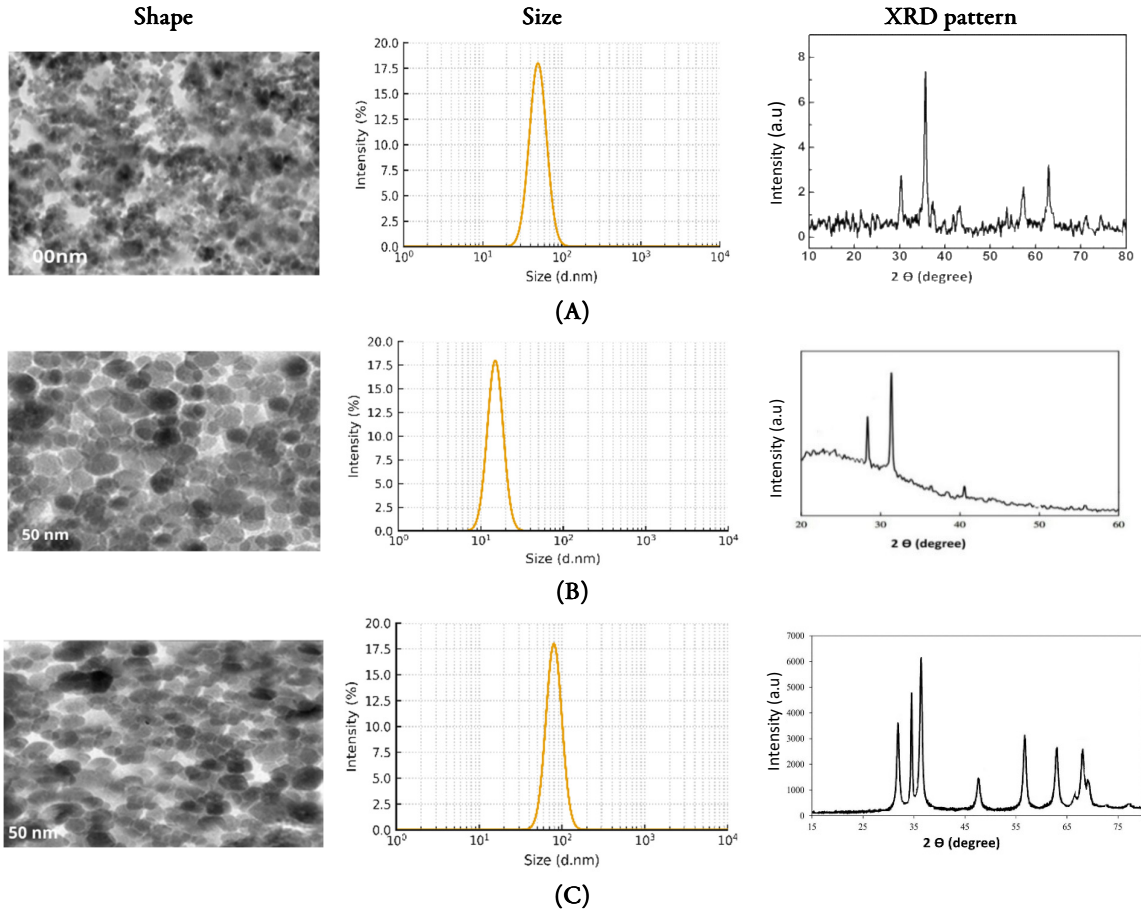

Figure 1. Characterization of Fe_3O_4NPs (A), MnO NPs (B), and ZnO NPs (C): shape, size, and XRD pattern analysis indicating the formation of nanoparticles

Table 2. Effect of some microelement nanoparticles on peanut pod rot diseases under greenhouse conditions

Micro-elements	Conc.	Pod rot incidence (%)			Apparent healthy (%)
		Dry brown lesion	Pink discoloration	General breakdown	
Fe_3O_4NPs	25	14.63cd*	1.59ab	15.30cde	68.48e
	50	13.08de	1.02ab	13.41ef	72.49c
	100	12.20ef	0.00b	12.22fg	75.58b
MnO NPs	25	16.88ab	2.55a	18.07ab	62.50f
	50	15.12bcd	1.96ab	15.77cd	67.15e
	100	12.96de	1.85ab	14.39def	70.80cd
ZnO NPs	25	18.37a	3.00a	18.60ab	60.03g
	50	16.25abc	2.29a	17.04bc	64.42f
	100	14.45cd	1.78ab	14.66de	69.11de
Baler		10.00f	0.00b	10.56g	79.44a
Control		17.85a	3.08a	19.72a	59.35g

*Means In each column with the same letter are not significantly different according to Duncan's Multiple Range Test ($P < 0.05$)

Among the treatments, Fe_3O_4 nanoparticles were the most effective, particularly at a concentration of 100 mg L, which resulted in the lowest overall pod rot incidence (12.22%) and the highest percentage of apparently healthy pods (75.58%). MnO and ZnO nanoparticles followed a similar trend, though their effects were slightly less pronounced, especially at lower concentrations. Notably, ZnO NPs at 25 mg L^{-1} recorded the highest pod rot incidence among all nanoparticle treatments (18.60%) and the lowest percentage of healthy pods (60.03%). The chemical fungicide (Baler), used as a positive control, exhibited the highest overall efficacy, achieving the lowest incidence of dry brown lesions (10.56%) and the highest percentage of healthy pods (79.44%).

Furthermore, the data clearly indicate a positive correlation between increasing nanoparticle concentrations and their effectiveness in reducing disease incidence. Statistical analysis confirmed that these differences were significant at the 5% level.

Effect of some microelement nanoparticles on the frequency of *Aspergillus flavus, A. parasitic, and* the amount of aflatoxin

The results presented in Table 3 clearly indicate that Fe_3O_4 NPs and MnO NPs, particularly at higher concentrations, were effective in reducing both fungal frequency and aflatoxin production compared to the untreated control. In particular, Fe_3O_4 NPs exhibited the highest efficacy compared to other nanoparticle microelements, especially at a concentration of 100 mg L^{-1}, where the frequencies of *Aspergillus flavus* and *A. parasiticus* decreased to 20% and 15%, respectively, when co-inoculated. Most notably, aflatoxin B_1 and B_2 levels were reduced to 33 ppb and 0.0 ppb, respectively.

Table 3. Effect of some microelement nanoparticles on the frequency of *Aspergillus flavus*, *A. parasiticus*, and aflatoxin contaminations in seed under greenhouse conditions

Micro-elements	Con. mg L^{-1}	*Aspergillus flavus*			*Aspergillus parasiticus*			*A. flavus* + *A. parasiticus*			
		A. flavus (%)	Content of aflatoxin (ppb)		*A. parasiticus* (%)	Content of aflatoxin (ppb)		*A. flavus* (%)	*A. parasiticus* (%)	Content of aflatoxin (ppb)	
			B_1	B_2		B_1	B_2			B_1	B_2
Fe_3O_4NPs	25	30	45	30	25	35	20	25	20	65	30
	50	25	38	15	25	20	0	20	15	42	18
	100	20	0	0	20	0	0	20	15	33	0
MnO NPs	25	40	55	30	20	50	22	35	20	75	35
	50	35	35	20	20	39	15	25	15	45	26
	100	25	30	0	15	0	0	20	15	40	15
ZnO NPs	25	35	70	35	35	65	35	35	30	66	34
	50	30	45	30	30	45	30	25	25	48	28
	100	50	90	45	45	80	42	45	30	110	45
Baler		10	0	0	15	0	0	15	15	20	0
Control		45	80	35	35	70	35	40	30	85	40

In the same way, MnO NPs give vigorous antifungal activity at 100 mg L^{-1}, with a noticeable reduction in fungal incidence and significant suppression of aflatoxin levels (B_1: 40 ppb, B_2: 15 ppb). While, in contrast, ZnO NPs showed less consistent performance. At the highest tested concentration (100 mg L^{-1}), the frequencies of *A. flavus* and *A. parasiticus* increased to 45% and 30%, respectively, and aflatoxin levels peaked at 110 ppb for B_1 and 45 ppb for B_2, surpassing even the control values (B_1: 85 ppb, B_2: 40 ppb).

The chemical fungicide (Baler), used as a positive control, was the most effective treatment overall, reducing aflatoxin B_1 and B_2 levels to 20 ppb and 0.0 ppb, respectively, and lowering fungal frequencies to 15% for both species under co-inoculation. Additionally, the data indicate a positive correlation between increasing concentrations of Fe_3O_4 NPs and MnO NPs and their effectiveness in reducing fungal frequency and aflatoxin

production. In contrast, ZnO NPs exhibited a negative trend, with higher concentrations leading to reduced efficacy.

The 3D surface plot illustrates the simultaneous distribution of Aflatoxin B_1 and B_2 concentrations across three nanoparticle treatments (Fe_3O_4, MnO, and ZnO) at varying doses (25, 50, and 100 mg L^{-1}). The surface for Aflatoxin B_1 peaks at approximately 110 ppb under the 100 mg L^{-1} ZnO treatment, whereas Fe_3O_4 nanoparticles at 25 mg L^{-1} result in a moderate level of around 65 ppb. In contrast, the B_2 surface begins with a relatively high concentration (~34 ppb) at 25 mg L^{-1} ZnO, drops to zero with 100 mg L^{-1} Fe_3O_4 NPs, and then rises again to approximately 45 ppb at 100 mg L^{-1} ZnO. This topographic variation reflects the complex interaction between nanoparticle type and concentration, emphasizing the importance of optimizing treatment parameters to minimize aflatoxin contamination while preserving biochemical efficacy (Figure 2).

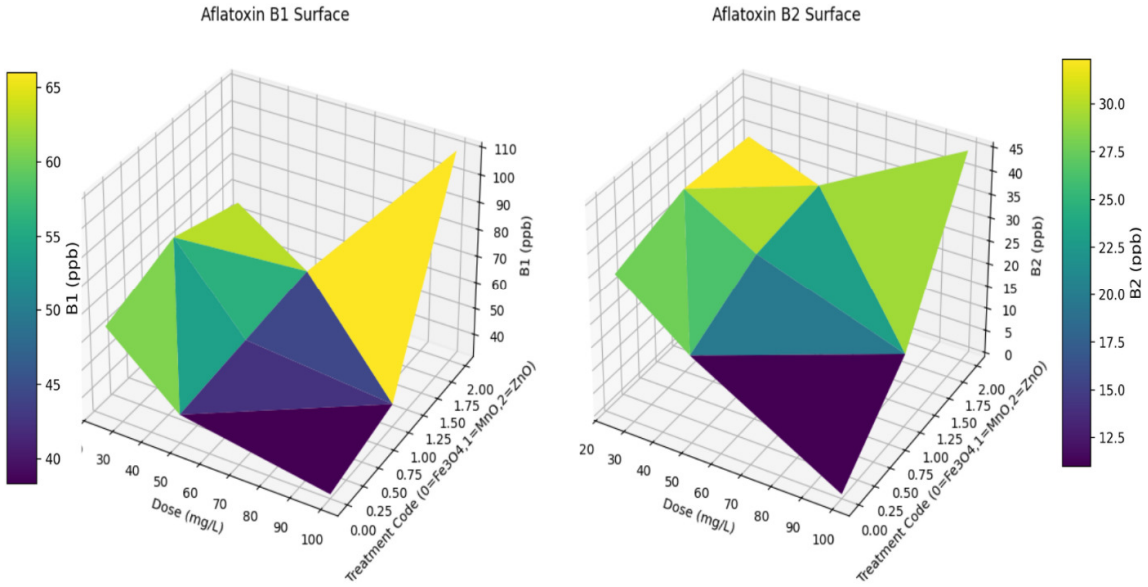

Figure 2. Three-dimensional surface plots showing Aflatoxin B_1 and B_2 concentrations in peanut seeds as functions of nanoparticle treatment (Fe_3O_4NPs, MnO NPs, ZnO NPs) and dose (25, 50, 100 mg L^{-1})

Figure 3's dual contour plots further delineate the distribution patterns of Aflatoxin B_1 and B_2 across the different nanoparticle treatments and concentrations. The B_1 plot (left panel) shows a steady decline in toxin levels with increasing Fe_3O_4 NP concentration, reaching minimal levels at 100 mg L^{-1}. In contrast, ZnO NPs produce a sharp increase in B_1 levels at the highest dose. The B_2 plot (right panel) reveals moderate suppression under Fe_3O_4 and MnO NPs, but a dose-dependent resurgence under ZnO NPs. The smooth gradient transitions in the contour maps underscore that high-dose Fe_3O_4 NPs provide the most consistent and effective reduction in both B_1 and B_2 aflatoxins. Conversely, ZnO NPs require precise dosage control to avoid unintended increases in aflatoxin accumulation.

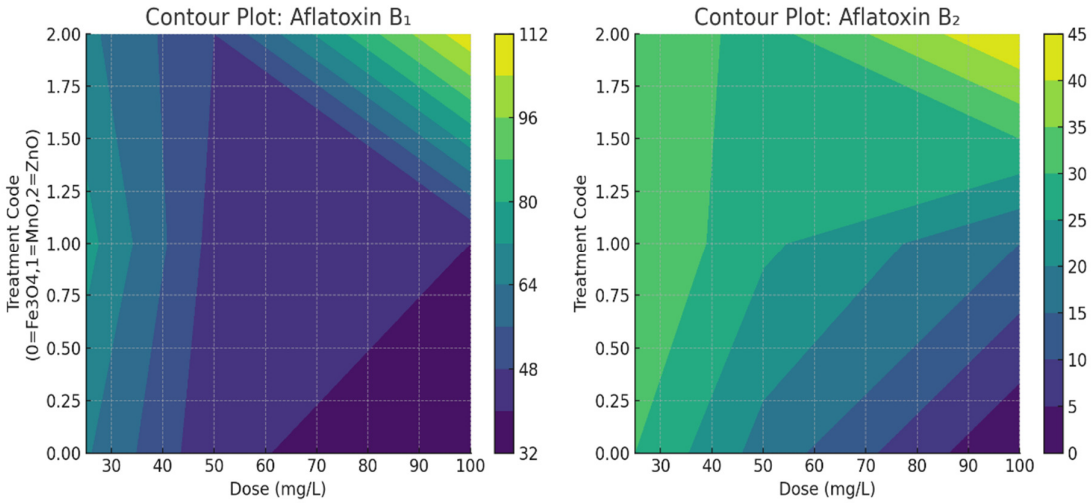

Figure 3. Contour plots of Aflatoxin B_1 and B_2 concentrations by nanoparticle treatment and dose

Field experiments

Effect of some micronutrient nanoparticles on peanut pod rot diseases

The present data in Table 4 illustrate the impact of micronutrient nanoparticles on peanut pod rot incidence under field conditions during the 2022 and 2023 growing seasons. The results reveal a consistent trend across both seasons, with all nanoparticle treatments leading to significant reductions in disease incidence and corresponding increases in the percentage of apparently healthy pods when compared to the untreated control.

Table 4. Effect of some micronutrient nanoparticles on peanut pod rots diseases under field conditions during the two growing seasons 2022 and 2023

Seasons		2022				2023			
Micro-elements	Con. mg L^{-1}	Pod rot incidence (%)			Apparent healthy (%)	Pod rot incidence (%)			Apparent healthy (%)
		Dry brown lesion	Pink dis-coloration	General break -down		Dry brown lesion	Pink dis-coloration	General break -down	
Fe_3O_4NPs	25	10.10bc*	0.17e	13.56bc	76.17cde	8.94b	0.70d	12.05b	78.31cd
	50	8.47cd	0.00f	12.39cd	79.14abc	7.27bc	0.47f	10.69bcd	81.57abc
	100	8.60cd	0.00f	10.20e	81.20ab	5.99cd	0.00h	9.32bcd	84.69cd
MnO NPs	25	11.96b	0.62c	13.81bc	73.61e	8.45b	0.69d	12.59b	78.27cd
	50	9.80bc	0.38d	12.51bcd	77.31bcde	7.55bc	0.07g	12.02b	80.36bcde
	100	8.88cd	0.00f	11.09de	80.03abc	6.78bc	0.00h	10.62bcd	82.60bcd
ZnO NPs	25	10.20bc	0.82b	14.81b	74.17de	9.06b	1.56b	11.86b	77.52d
	50	9.58c	0.63c	13.29bcd	76.50cde	7.81bc	1.00c	11.54bc	79.65cd
	100	8.12cd	0.62c	12.62bcd	78.64bcd	6.95bc	0.62e	10.87bc	81.56bcd
Baler		6.92d	0.00f	9.57e	83.51a	4.63d	0.00h	8.45d	86.92a
Control		14.08a	1.33a	17.62a	66.97f	11.19a	2.30a	15.42a	71.09e

*Means In each column with the same letter are not significantly different according to Duncan's Multiple Range Test ($P < 0.05$)

From the nanoparticle treatments, Fe_3O_4 NPs demonstrated the most pronounced and stable effect. At the highest concentration (100 mg L^{-1}), Fe_3O_4 NPs give the lowest pod rot incidence, recorded at 10.20% in 2022 and 9.32% in 2023, alongside the highest percentages of healthy pods (81.20% and 84.69%, respectively).

While MnO NPs showed strong efficacy, particularly at 100 mg L^{-1}, where disease incidence was reduced to 11.09% in 2022 and 10.62% in 2023, while healthy pod percentages reached 80.03% and 82.60%, respectively. Although ZnO NPs exhibited slightly lower effectiveness, it still outperformed the untreated control. At 100 mg L^{-1}, Zn treatment reduced disease incidence to 12.62% and 10.87% in 2022 and 2023, respectively. Moreover, the data clearly indicate a positive correlation between increasing nanoparticle concentrations and their effectiveness in reducing disease incidence. On the other hand, chemical fungicide (Baler), which was used as a positive control, consistently showed the highest protective effect, achieving the lowest disease incidence in both seasons (9.57% in 2022, 8.45% in 2023) and the highest proportions of healthy pods (83.51% and 86.92%, respectively).

Effect of some micronutrient nanoparticles on the frequency of *Aspergillus flavus*, *A. parasiticus*, and the amount of aflatoxin

Data obtained in Table 5 presents the effect of micronutrient nanoparticles on the frequency of *Aspergillus flavus and A. parasiticus*, along with their associated aflatoxin B_1 and B_2 contamination in peanut seeds under field conditions during the 2022 and 2023 growing seasons. The data clearly indicate that all nanoparticle treatments reduced fungal infection and aflatoxin accumulation to varying degrees, depending on the element type and applied concentration.

Table 5. Effect of some micronutrient nanoparticles on the frequency of *Aspergillus flavus*, *A. parasiticus*, and aflatoxin contaminations in seed under field conditions during the two growing seasons 2022 and 2023

Seasons		2022				2023			
Micronutrient	Con. (mg L^{-1})	*A. flavus* (%)	*A. parasiticus* (%)	Content of aflatoxin (ppb)		*A. flavus* (%)	*A. parasiticus* (%)	Content of aflatoxin (ppb)	
				B_1	B_2			B_1	B_2
Fe_3O_4NPs	25	25	15	75	18	15	10	45	18
	50	20	10	30	15	10	10	20	0
	100	10	0	0	0	10	0	0	0
MnO NPs	25	30	20	87	32	25	20	67	25
	50	25	10	67	0	20	15	32	15
	100	15	10	50	0	15	10	25	0
ZnO NPs	25	20	15	117	30	15	10	93	0
	50	30	20	130	47	20	20	120	30
	100	35	25	170	55	30	20	160	42
Baler		10	5	0	0	5	0	0	0
Control		30	20	137	47	25	20	112	30

Among the tested treatments, iron nanoparticles (Fe_3O_4 NPs) exhibited the most potent antifungal and antitoxigenic effects. At 100 mg L^{-1}, Fe_3O_4 NPs completely inhibited *A. parasiticus* in both seasons, and aflatoxins B_1 and B_2 were undetectable. Even at 50 mg L^{-1}, Fe_3O_4 NPs significantly reduced aflatoxin levels to trace or undetectable amounts. MnO NPs also showed effective control, particularly at 100 mg L^{-1}, where *A. flavus* and *A. parasiticus* frequencies were reduced to 15% or lower, and aflatoxin B_2 was suppressed entirely in both years. Aflatoxin B_1 levels were also significantly reduced under Mn treatment.

In contrast, ZnO NPs exhibited an adverse trend at higher concentrations. At 100 mg L^{-1}, they failed to control *A. flavus* and *A. parasiticus* frequency, and instead resulted in the highest aflatoxin contamination recorded across both seasons. In 2022, aflatoxin B_1 and B_2 reached 170 ppb and 55 ppb, respectively, while in 2023, they remained high at 160 ppb (B_1) and 45 ppb (B_2), exceeding even the values observed in the untreated control. While the positive control (Baler) consistently demonstrated high efficacy, with the lowest fungal incidence and undetectable levels of aflatoxins in both seasons, confirming its strong protective role.

Effect of some micronutrient nanoparticles on total peanut pod yield

The results presented in Table 6 illustrate the impact of micronutrient nanoparticles on total peanut pod yield and the percentage increase relative to the untreated control under field conditions during the 2022 and 2023 growing seasons. The results clearly demonstrate that all micronutrient treatments contributed to a statistically significant improvement in yield, with Fe_3O_4 NP showing the most pronounced effect. At 100 mg L^{-1}, Fe_3O_4 NP achieved the highest pod yield in both years, 1.550 tons/fed in 2022 and 1.509 tons/fed in 2023, corresponding to yield increases of 36.80% and 34.73%, respectively, compared to the control. Even at lower concentrations, Fe_3O_4 NP consistently outperformed manganese MnO NPs and ZnO NPs.

Table 6. Effect of some micronutrient nanoparticles on total peanut pod yield and yield increase percentage under field conditions during the two growing seasons 2022 and 2023

Seasons		2022		2023	
Micro-elements	**Con. (mg L^{-1})**	**Pod yield Ton/fed**	***Increases (%)**	**Pod yield Ton/fed**	***Increases (%)**
Fe_3O_4NPs	25	1.405ab**	24.01	1.390abcd	24.11
	50	1.510ab	33.27	1.426abc	27.32
	100	1.550a	36.80	1.509ab	34.73
MnO NPs	25	1.260ab	11.21	1.220cd	8.93
	50	1.286ab	13.50	1.253bcd	11.88
	100	1.310ab	15.62	1.286abcd	14.82
ZnO NPs	25	1.336ab	17.92	1.266bcd	13.04
	50	1.390ab	22.68	1.326abcd	18.39
	100	1.400ab	24.45	1.376abcd	22.86
Baler		1.616a	42.63	1.563a	39.55
Control		1.133b	0.00	1.120d	0.00

*Increases related to the control; **Means In each column with the same letter are not significantly different according to Duncan's Multiple Range Test ($P < 0.05$)

Data also indicated that, ZnO NPs enhanced yield in a dose-dependent manner, reaching 1.410 tons/fed (24.45% increase) in 2022 and 1.376 tons/fed (22.86% increase) in 2023 at 100 mg L^{-1} while, MnO NPs, effective, showed more modest improvements, with maximum yields of 1.310 and 1.286 tons/fed, corresponding to 15.62% and 14.82% increases in 2022 and 2023, respectively. However, the chemical fungicide Baler remained the top-performing treatment overall, achieving the highest yields, 1.616 tons/fed (42.63% increase) in 2022 and 1.563 tons/fed (39.55%) in 2023. In contrast, the untreated control recorded the lowest yields (1.133 and 1.120 tons/fed), serving as the baseline for comparison during the 2022 and 2023 growing seasons.

Biochemical changes associated with micronutrient nanoparticle treatments

The effect of different microelement nanoparticles on various biochemical changes, i.e., phenol content, activity of oxidative enzymes, reducing and sugar content, total free amino acids, and percentage of protein content, was studied.

Effect of micronutrient nanoparticles on phenol contents

Data in Table 7 presents the effect of micronutrient nanoparticles on the accumulation of phenolic compounds in 15-day-old primordial peanut pods. The results indicate that all nanoparticle treatments significantly enhanced both free and conjugated phenol contents compared to the untreated control and the chemical fungicide treatment (Baler).

Data also show that Fe_3O_4 NPs had the most pronounced effect, with total phenol content increasing progressively with concentration, reaching a maximum of 19.86 mg g^{-1} fresh weight. This increase was primarily attributed to elevated levels of both free phenols (13.88 mg g^{-1}) and conjugated phenols (5.98 mg g^{-1}). While

ZnO NPs also demonstrated a strong stimulatory effect, with total phenol content reaching 18.03 mg g^{-1}, followed by MnO NPs, which recorded a maximum value of 14.37 mg g^{-1} at the same concentration.

Table 7 Effect of some micronutrient nanoparticles on phenol contents in primordial pods (15-day-old) of peanut plants

Microelements	Con. (mg L^{-1})	Phenol content (mg g^{-1} fresh weight)		
		Free	Conjugate	Total
Fe_3O_4NPs	25	10.21cd*	4.45abcd	14.66de
	50	12.01abc	5.61ab	17.62bc
	100	13.88a	5.98a	19.86a
MnO NPs	25	6.33fe	2.36d	8.69g
	50	7.91e	3.71bcd	11.62f
	100	10.55bc	3.82abcd	14.37de
ZnO NPs	25	8.22de	4.24abcd	12.46fe
	50	10.73bc	4.88abc	15.61cd
	100	12.68ab	5.35ab	18.03ab
Baler		4.14fg	3.55bcd	7.69hg
Control		3.31g	3.12cd	6.43h

*Means In each column with the same letter are not significantly different according to Duncan's Multiple Range Test ($P < 0.05$)

Notably, even at the lowest concentration (25 mg L^{-1}), all nanoparticle treatments led to substantial increases in total phenol content compared to both the control and fungicide treatment, which recorded 6.43 mg g^{-1} and 7.69 mg g^{-1}, respectively. Furthermore, the data reveal a clear positive relationship between increasing nanoparticle concentrations and the accumulation of phenolic compounds in peanut tissues.

Effect of some micronutrient nanoparticles on peroxidase, polyphenoloxidase, and catalase activity

The results presented in Table 8 demonstrate the significant impact of micronutrient nanoparticles on the activity of three key defense-related enzymes: peroxidase (PO), polyphenol oxidase (PPO), and catalase (CAT) in 15-day-old primordial peanut pods. All nanoparticle treatments significantly increased the activities of these enzymes compared to both the untreated control and the chemical fungicide treatment (Baler), indicating an enhancement of the plant's physiological defense mechanisms.

Table 8. Effect of some micronutrient nanoparticles on peroxidase, polyphenoloxidase, and catalase activity in primordial pods (15-day-old) of peanut plants

Micronutrients	Con. (mg L^{-1})	Enzyme activity		
		Peroxidase (PO)	Polyphenoloxidase (PPO)	Catalase (CAT)
Fe_3O_4NPs	25	0.662abc*	1.740abc	0.529a
	50	0.743ab	1.825ab	0.590a
	100	0.810a	1.890a	0.663a
MnO NPs	25	0.448cd	1.541cde	0.407ab
	50	0.462cd	1.552cde	0.449ab
	100	0.505bcd	1.560cd	0.461ab
ZnO NPs	25	0.457cd	1.550cdf	0.447ab
	50	0.486bcd	1.566cd	0.461ab
	100	0.552bcd	1.580bcd	0.474ab
Baler		0.385d	1.358de	0.231b
Control		0.311d	1.301e	0.252b

*Means in each column with the same letter are not significantly different according to Duncan's Multiple Range Test ($P < 0.05$)

In this regard, Fe_3O_4 NPs showed the most pronounced effect, with enzymatic activity increasing progressively with concentration. At the highest concentration (100 mg L^{-1}), Fe_3O_4 NPs induced the greatest activities, reaching 0.810 U/mg for PO, 1.890 U/mg for PPO, and 0.663 U/mg for CAT. ZnO NPs also displayed substantial stimulatory effects at 100 mg L^{-1}, with corresponding enzyme activities of 0.552 U/mg (PO), 1.580 U/mg (PPO), and 0.474 U/mg (CAT). Similarly, MnO NPs resulted in notable increases, recording 0.505, 1.560, and 0.461 U/mg for PO, PPO, and CAT, respectively.

In contrast, the chemical fungicide Baler showed only moderate induction of enzyme activity (PO: 0.385, PPO: 1.358, CAT: 0.231 U/mg), while the untreated control recorded the lowest values across all enzymatic parameters. Overall, the data suggest a positive dose-dependent relationship between nanoparticle concentration and the activation of plant defense enzymes, particularly with Fe_3O_4 and ZnO nanoparticles.

Effect of some micronutrient nanoparticles on sugar content and total free amino acids

Data in Table 9 show the effects of micronutrient nanoparticles on the biochemical composition of 15-day-old primordial peanut pods, with a focus on sugar fractions, free amino acids, and total protein content. The results indicate that nanoparticle treatments, particularly with iron (Fe_3O_4 NPs), significantly enhanced key metabolic indicators associated with plant vigor, early development, and defense readiness.

Table 9 Effect of some micronutrient nanoparticles on sugar content and total free amino acids in primordial pods (15-day-old) of peanut plants

Micro-elements	Con. (mg L^{-1})	Sugars content (mg g^{-1} fresh weight)			Free amino acids (mg g^{-1} fresh weight)	Protein content (%)
		Reducing	Non-reducing	Total		
Fe_3O_4NPs	25	7.23e*	1.12cd	8.35f	0.712abcd	10.84f
	50	8.47c	1.33bc	9.80d	0.734abc	12.85c
	100	10.95a	1.15bcd	12.10a	0.904a	14.33a
MnO NPs	25	6.74f	1.05d	7.79g	0.474d	10.21g
	50	8.36cd	1.16bcd	9.52e	0.710abcd	11.57e
	100	9.57b	1.34bc	10.91c	0.791abc	13.40b
ZnO NPs	25	6.23g	1.24bcd	7.47h	0.553cd	10.24g
	50	8.11d	1.25bcd	9.36e	0.651abcd	11.97d
	100	9.80b	1.40b	11.20b	0.891a	13.58b
Baler		6.10g	1.24bcd	7.34h	0.635bcd	1.36i
Control		4.70h	1.99a	6.69i	0.581cd	8.22h

*Means in each column with the same letter are not significantly different according to Duncan's Multiple Range Test ($P < 0.05$)

Data also illustrate that, at a concentration of 100 mg L^{-1}, Fe_3O_4 nanoparticles induced the highest levels of all measured biochemical parameters, including total sugars (12.10 mg g^{-1} fresh weight), free amino acids (0.904 mg g^{-1}), and protein content (14.33%), reflecting a potent stimulatory effect on primary metabolism. In the same way, ZnO and MnO nanoparticles also improved biochemical composition compared to both the untreated control and the fungicide treatment (Baler), though to a lesser extent than iron. In this respect, at 100 mg L^{-1}, ZnO NPs resulted in 11.20 mg g^{-1} total sugars, 0.891 mg g^{-1} free amino acids, and 13.58% protein content, while MnO NPs recorded 10.91 mg g^{-1}, 0.791 mg g^{-1}, and 13.40%, respectively. In contrast, both the Baler treatment and the untreated control exhibited the lowest value.

This PCA biplot (Figure 4) succinctly captures the multivariate biochemical shifts induced by nanoparticle treatments. Principal Component 1 (accounting for ≈45 % of variance) separates high-phenol and catalase-rich treatments (notably 100 mg L^{-1} Fe_3O_4NPs) to the right from sugar- and protein-dominated treatments (mid-dose MnO and ZnO NPs) on the left. Principal Component 2 (≈25 % of variance) distinguishes peroxidase- and PPO-enriched treatments (low-dose Fe_3O_4NPs) toward the top from treatments with lower enzymatic activity toward the bottom. The clear clustering of treatments demonstrates dose-

dependent metabolic reprogramming, validating that Fe_3O_4NPs at high concentration maximize phenolic defenses, whereas MnO and ZnO elicit balanced osmoprotective responses.

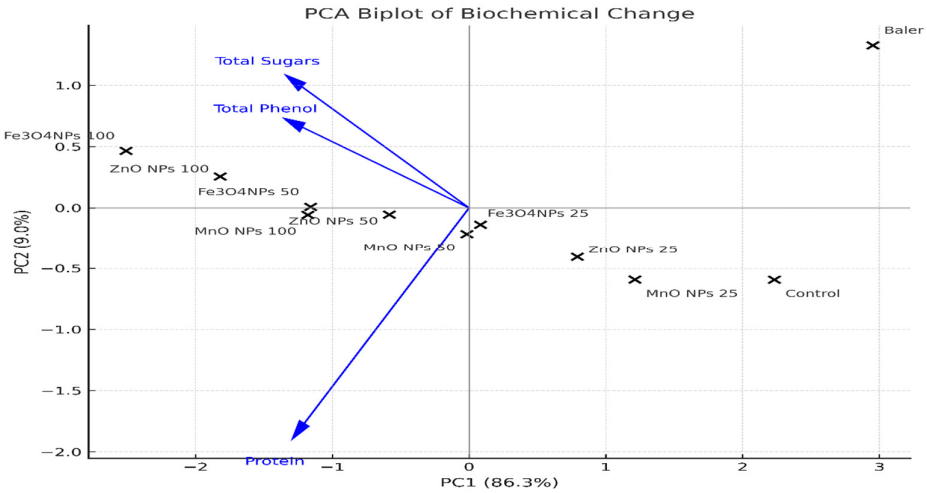

Figure 4. Principal component analysis (PCA) of biochemical changes in peanut samples treated with Fe_3O_4 NPs, MnO NPs, and ZnO NPs at doses of 25, 50, and 100 mg L^{-1}

The heatmap of biochemical changes (Figure 5) illustrates the differential responses of chamomile plants to various concentrations of Fe_3O_4, MnO, and ZnO nanoparticles. Notably, treatment with Fe_3O_4 NPs at 100 mg L^{-1} resulted in the highest accumulation of total phenols, as indicated by the intense red coloration, suggesting enhanced activation of phenolic-based defense pathways.

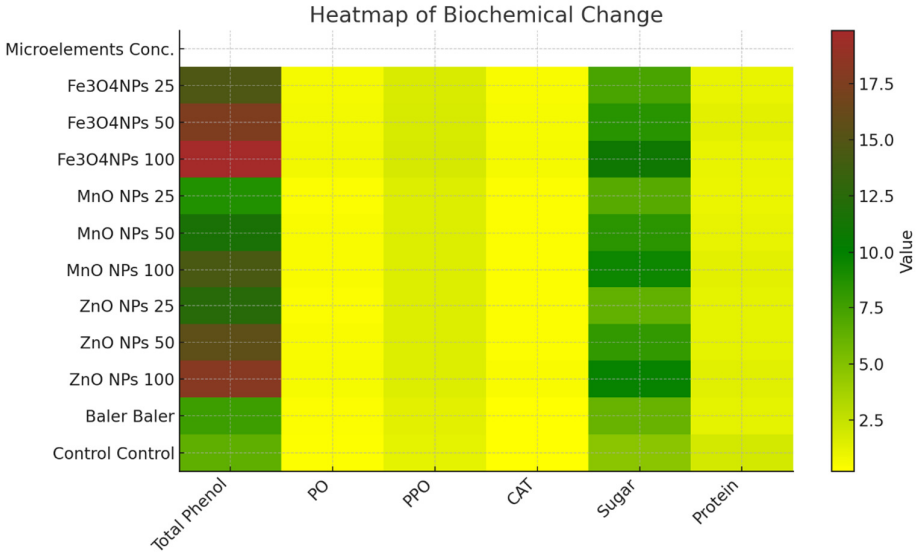

Figure 5. Heatmap illustrating dose-dependent biochemical changes in peanut pods treated with Fe_3O_4, MnO, and ZnO nanoparticles (25, 50, 100 mg L^{-1}), showing total phenolic content, enzyme activities (PO, PPO, CAT), sugar, and protein responses

Moderate variations were observed in the activities of key antioxidant enzyme (PO, PPO, and CAT) across all treatments, with most values clustering within the yellow range, indicating relatively uniform enzymatic responses. Soluble sugar content increased significantly under MnO and Fe_3O_4 treatments,

especially at higher doses, reflecting possible stimulation of metabolic activity and stress adaptation. In contrast, protein levels remained largely stable across treatments, with minimal fluctuation from the control. Both the control and Baler treatments exhibited lower biochemical activity, particularly in total phenol and sugar content, highlighting the superior biochemical enhancement conferred by nanoparticle applications, especially Fe_3O_4 at 100 mg L^{-1}.

Discussion

In light of the pressing need to combat climate change and its disruptive effects on biological systems and in response to the growing demand for safe, fungicide-free food with minimal environmental impact, the development of innovative plant disease resistance strategies has become imperative. These strategies focus on strengthening the plant's innate defense mechanisms by inducing physiological changes that enhance its resilience to pathogens. Among the most promising of these approaches is the use of micronutrients, particularly in their nanoparticle form, as inducers of resistance. Accordingly, the present study evaluated the effectiveness of micronutrient nanoparticles in managing peanut pod rots, the occurrence of aflatoxigenic fungi, and the amount of aflatoxin

The results illustrated that all tested treatments significantly reduced disease incidence, the frequency of aflatoxigenic fungi, and the amount of aflatoxin in greenhouse experiments conducted under artificial inoculation. These findings were consistent with those obtained from field experiments under natural inoculation conditions during the 2022 and 2023 growing seasons, compared to the untreated control. In this regard, Fe_3O_4 nanoparticles at 100 mg L^{-1} exhibited the highest efficacy in lowering pod rot disease incidence as well as an increase in pod yield, followed by MnO NPs at 100 mg L^{-1} and Zn NPs at 100 mg L^{-1}. While Baler fungicide, as expected, yielded the highest productivity and efficacy in disease control, Fe_3O_4 NPs proved to be a strong alternative with nearly comparable effects. On the other hand, results indicated that Zn NPs in high concentration make peanut pods more susceptible to invasion by aflatoxigenic fungi and increase their aflatoxin content. This is in agreement with Payne and Brown (1998), Emara *et al.* (2004), and Mahmoud *et al*. (2009) who stated that Zn played an important role in the regulation of aflatoxin production and supplementation of Zn performed to the activity of fatty acid synthetase (FAS), which corresponded to aflatoxin B1 biosynthesis.

In agreement with recent investigations, our 3D surface analysis reveals a nuanced, dose-dependent modulation of Aflatoxin B_1 and B_2 levels influenced by nanoparticle type. Specifically, the pronounced peak of B_1 at 100 mg L^{-1} ZnO is consistent with the findings of Zhang *et al.* (2023), who reported that high concentrations of zinc oxide nanoparticles can stimulate aflatoxin biosynthesis. Conversely, the marked reduction of B_2 levels under Fe_3O_4NP treatment aligns with observations by Kumar and Ahmed (2023), highlighting the potential of iron oxide nanoparticles to suppress aflatoxin B_2 production. The moderate elevations observed for both B_1 and B_2 under MnO NP treatments corroborate the findings of Gonçalves *et al.* (2021), who indicated that manganese oxide nanoparticles may modulate both primary metabolism and defense responses. Collectively, these findings underscore the importance of carefully optimizing nanoparticle composition and concentration to effectively reduce aflatoxin contamination while maintaining or enhancing plant physiological performance.

The present study demonstrated that the application of micronutrient nanoparticles, particularly Fe_3O_4 NPs at 100 mg L^{-1}, significantly enhanced the biochemical and metabolic responses of peanut plants under pathogenic stress. The marked increase in phenolic compound content and the elevated activities of catalase (CAT), peroxidase (PO), and polyphenol oxidase (PPO) observed in peanut primordial pods suggest that Fe_3O_4 nanoparticles effectively triggered the plant's antioxidative defense system. These enzymes are widely recognized as central components of the reactive oxygen species (ROS) scavenging network, which mitigates cellular damage during pathogen invasion.

In addition to activating antioxidant enzymes, Fe_3O_4 NPs also stimulated significant increases in total soluble sugars, free amino acids, and protein levels. These biochemical changes reflect enhanced metabolic activity and resource allocation toward stress adaptation and defense, consistent with the concept of "priming", wherein treated plants exhibit an elevated baseline resistance state. This priming effect may contribute not only to improved disease resistance but also to better growth and yield performance under stress conditions.

Although ZnO and MnO NPs also induced defense-related responses, their effects were comparatively lower than those of Fe_3O_4 NPs. This suggests that iron nanoparticles may possess a more potent or broader spectrum of bioactivity in modulating plant defense pathways.

Iron is an essential micronutrient involved in a variety of physiological processes, including chlorophyll synthesis and electron transport, and it serves as a cofactor in enzymes required for lignin biosynthesis and nitrogen metabolism (Pahlsson, 2004; Sirelkhatim *et al*., 2015; Zafar *et al*., 2016; Tsewang *et al*., 2024).

These findings are in agreement with previous studies reporting the role of micronutrients in activating plant defense mechanisms. Mahmoud *et al*. (2009) found that micronutrient treatments enhanced the activity of key enzymes such as ascorbic acid oxidase, peroxidase, and catalase, while also increasing the levels of phenolic compounds and phenol activity. These compounds and enzymes serve as biochemical markers of induced systemic resistance and play vital roles in strengthening plant cell walls, detoxifying ROS, and inhibiting pathogen proliferation (Zafar *et al*., 2016; García-López *et al*., 2018).

The gradient patterns observed in the heatmap support recent findings that nanoparticle treatments modulate plant secondary metabolism and defense enzyme activities in a dose-dependent manner. Notably, there was a substantial increase in total phenolic content under high conditions. The observed increase under Fe_3O_4 NP application is consistent with the findings of Kumar and Ahmed (2023), who reported that iron oxide nanoparticles significantly enhance phenolic biosynthesis in peanut tissues. Likewise, the elevated peroxidase (PO) and polyphenol oxidase (PPO) activities observed at lower nanoparticle concentrations align with the observations of Zhang *et al*. (2023), who demonstrated that low-dose nanoparticle exposure can optimally stimulate antioxidant defense enzymes without triggering oxidative stress. Furthermore, the enhanced sugar and protein levels recorded under moderate MnO and ZnO NP treatments corroborate the nanoparticle-mediated metabolic balancing model proposed by Gonçalves *et al.* (2021) and Atwa *et al*. (2025). These results collectively underscore the potential of fine-tuning nanoparticle composition and dosage as a strategic approach to strengthen peanut biochemical defenses while maintaining metabolic homeostasis and enhancing nutritional quality.

Moreover, several studies have emphasized the broader physiological roles of micronutrients beyond disease resistance. Zinc is known to regulate protein, carbohydrate, nucleic acid, and lipid metabolism, while also contributing to enzyme activation and gene expression. Manganese participates in photosynthetic oxygen evolution and is involved in phenolic compound metabolism (Sirelkhatim *et al.,* 2015; Zafar *et al.,* 2016; García-López *et al.,* 2018; Salvia *et al.,* 2023; Tsewang *et al.,* 2024). The higher efficiency of nanoparticles compared to conventional formulations has been attributed to their small size and large surface area, which enhance their bioavailability, penetration into plant tissues, mobility within the plant system, and improve uptake and utilization, ultimately increasing nutrient use efficiency and bolstering disease resistance (Pan and Xing, 2012; An *et al.,* 2022; Vijayreddy *et al.,* 2023). The physicochemical characterization of the nanoparticles further supports these findings. High-resolution TEM images confirmed the nearly spherical morphology of all nanoparticles, with average sizes of 55 ± 19 nm (Fe_3O_4), 15 ± 22 nm (MnO), and 85 ± 12 nm (ZnO). XRD analysis further validated the crystalline nature of the nanoparticles, confirming the formation of magnetite (Fe_3O_4), cubic MnO, and hexagonal wurtzite ZnO structures with high crystallinity and phase purity. Field-scale trials are required to validate the efficacy of these nanoparticles under variable agro-climatic conditions.

Finally, translation to practice should follow precautionary, risk-based frameworks (e.g., EFSA, OECD) that require nano-specific characterization (identity, dose, dispersion stability, particle-size metrics at the applied rate) and assessment of environmental fate and non-target exposure in relevant compartments. Given

that field evidence remains more limited than greenhouse data, we recommend staged adoption - from small-plot pilots to multi-location trials - accompanied by environmental monitoring (residues, non-target indicators). Practical safeguards include using the minimum effective dose, adhering to PPE and buffer-zone practices, avoiding flowering and high-drift conditions, and verifying formulation quality at the point of use (e.g., DLS). Within this framework, Fe_3O_4 nanoparticles show strong field potential, warranting multi-season, multi-site validation across diverse agro-ecological settings.

Conclusion

Overall, Fe_3O_4 nanoparticles exhibited the most consistent and effective performance across all tested parameters, including disease suppression, aflatoxin control, yield improvement, and stimulation of biochemical defenses. MnO NPs were also effective, though to a lesser extent. In contrast, ZnO NPs demonstrated variable efficacy, with high concentrations showing potential adverse effects. These findings underscore the potential of micronutrient nanoparticles, particularly iron oxide, as promising, eco-friendly tools for enhancing crop health and productivity, provided their concentrations are carefully managed.

Authors' Contributions

Conceptualization: EM, ZNH, MIA, AEA, WS, SA, MAA; Data curation: EM, ZNH, MIA, AEA; Formal analysis: EM, ZNH, MIA, AEA, WS, SA, MAA; Funding acquisition: WS, SA Investigation: EM, ZNH, MIA, AEA, WS, SA, MAA; Methodology: EM, ZNH, MIA, AEA; Project administration: EM, WS, SA, MAA; Resources: EM, ZNH, MIA, AEA; Software: EM, ZNH, MIA, AEA; Supervision: EM; Validation: EM, ZNH; Visualization: EM, ZNH, MIA; Roles/Writing - original draft: EM, ZNH, MIA, AEA, WS, SA, MAA; and Writing - review & editing: EM, ZNH, MIA, AEA, WS, SA, MAA.

All authors read and approved the final manuscript.

Acknowledgements

We extend our thanks to the Deanship of Scientific Research, Vice Presidency for Graduate Studies and Scientific Research, King Faisal University, Saudi Arabia (Project No. KFU254031), for supporting this research work.

Funding

This work was supported by the Deanship of Scientific Research, Vice Presidency for Graduate Studies and Scientific Research at King Faisal University, Saudi Arabia, under Project No. KFU 254031.

Conflict of Interests

The authors declare that there are no conflicts of interest related to this article.

References

AOAC Association of Official Analytical Chemists (1998). Official methods of analysis of association of official analytical chemists international (16th ed). AOAC International. Arlington, VA, USA.

AOAC Association of Official Analytical Chemists (2000). Natural toxins. In: Official methods of association of official analytical chemists (17th ed). AOAC International. Washington, DC.

Atia AM, El-Khateeb EA, Abd El-Maksoud RM, Abou-Zeid MA, Salah A, Abdel-Hamid AME (2021). Mining of leaf rust resistance genes content in Egyptian bread wheat collection. Plants 10(7):1378. *https://doi.org/10.3390/plants10071378*

Atwa AA, Ahmed SS, Abd El-Aziz GH, Abou-Zeid MA, Omara RI, Atwa NA, Fahmy AH (2025). Leaf rust resistance in wheat and interpretation of the antifungal activity of silver and copper nanoparticles. Scientific Reports 15:9429. *https://doi.org/10.1038/s41598-025-91127-4*

Bediako KA, Ofori K, Offei SK, Dzidzienyo D, Asibuo JY, Amoah RA (2019). Aflatoxin contamination of groundnut (*Arachis hypogaea* L.): Predisposing factors and management interventions. Food Control 98(4):61-67. *https://doi.org/10.1016/j.foodcont.2018.11.020*

Emara MF, El-Deeb AA, Hamza S (2004). Effect of micronutrients and calcium nutrition on peanut yellow mold and aflatoxin content. Journal of Agricultural Science, Mansoura University 29(6):3153-3162. *https://journals.ekb.eg/article_238646_1c35a5c216cf0ff8308cf5f12ca1af1e.pdf*

FAO Food and Agriculture Organization of the United Nations (2024). FAOSTAT statistical database. FAO, Rome, Italy. *https://www.fao.org/faostat/en/*

Filonow AB, Melouk HA, Martin M (1988). Effect of calcium sulfate on pod rot of peanut. Plant Disease 72:589-593.

Fouda KF (2017). Response of onion yield and its chemical content to NPK fertilization and foliar application of some micronutrients. Egyptian Journal of Soil Science 56(3):549-561.

García-López JI, Zavala-García F, Olivares-Sáenz E, Lira-Saldívar RH, Díaz-Barriga-Castro E, Ruiz-Torres NA (2018). Zinc oxide nanoparticles boosts phenolic compounds and antioxidant activity of *Capsicum annuum* L. during germination. Agronomy 8(10):215. *https://doi.org/10.3390/agronomy8100215*

Garren KH, Porter DM (1970). Quiescent endocarp floral communities in cured mature peanuts from Virginia and Puerto Rico. Phytopathology 60:1635-1638.

Goldschmidt EE, Goren R, Monselise SP (1968). The IAA oxidase system of citrus roots. Planta 72:213-222.

Gonçalves S, Mansinhos I, Rodríguez-Solana R, Pereira-Caro G, Moreno-Rojas JM, Romano A (2021). Impact of metallic nanoparticles on in vitro culture, phenolic profile and biological activity of two Mediterranean Lamiaceae species: *Lavandula viridis* L'Hér and *Thymus lotocephalus* G. López and R. Morales. Molecules 26(21):6427. *https://doi.org/10.3390/molecules26216427*

He W, Feng L, Li Z, Zhang K, Zhang Y, Wen XI, Sun WM (2022). *Fusarium neocosmosporiellum* causing peanut pod rot and its biological characteristics. Acta Phytopathologica Sinica 52:493-498.

Hussien ZN, Gomaa AM (2020). Integration between antagonistic fungi and bacteria for controlling peanut pod rot incidence and occurrence of aflatoxigenic fungi. Middle East Journal of Applied Sciences 10(4):638-648. *https://doi.org/10.36632/mejas/2020.10.4.54*

Kankam F, Larbi-Koranteng S, Sowley EK (2021). Aflatoxin contamination in groundnut (*Arachis hypogaea* L.): Its causes and management. Ghana Journal of Science, Technology and Development 7(2):102-121. *https://doi.org/10.47881/264.967x*

Kumar P, Ahmed S (2023). Effects of iron oxide nanoparticles on phenolic accumulation and antioxidative enzymes in *Arachis hypogaea*. Plant Physiology and Biochemistry 180:342-350.

Liu Y, Xiukun L, Yiming F, Lifeng L, Limin S, Geng Y, Yuhong G, Zhang Y (2024). Classification of peanut pod rot based on improved YOLOv5s. Frontiers in Plant Science 15:1364185. *https://doi.org/10.3389/fpls.2024.1364185*

Mahmoud EY, Gomaa MA (2015). Impact of some essential plant oils for controlling peanut pod rot diseases and aflatoxin. Journal of Biological Chemistry & Environmental Sciences 10(1):261-280.

Mahmoud EY, Hussien ZN, Yousef HR, Fatouh HM (2024). Comparison between some biotic and abiotic inducers in controlling peanut pod rots and aflatoxin contamination. Egyptian Journal of Phytopathology 52(2):113-126. *https://doi.org/10.13140/RG.2.2.15731.44326*

Mahmoud EY, Saleh WAM, Marei TA (2009). Efficiency of microelements as inducer resistance factor of peanut pod rot diseases and aflatoxigenic fungi. Egyptian Journal of Applied Sciences 24(4A):91-110.

Maren AK, Johan IP (1988). A laboratory guide to the common *Aspergillus* species and their teleomorph. Division of Food Processing, Commonwealth Scientific and Industrial Research Organization Division of Food Research, North Ryde.

Moore S, Stein WH (1954). A modified ninhydrin reagent for photometric determination of amino acids and related compounds. Journal of Biological Chemistry 211:907-913. *https://doi.org/10.1016/S0021-9258(18)71178-2*

Mueller S, Riedel H, Stremmel W (1997). Determination of catalase activity at physiological hydrogen peroxide concentrations. Analytical Biochemistry 245:55-60. *https://doi.org/10.1006/abio.1996.9939*

Omar HS, Al Mutery A, Osman NH, Reyad NE, Abou-Zeid MA (2021). Molecular marker analysis of stem and leaf rust resistance in Egyptian wheat genotypes and interpretation of the antifungal activity of chitosan-copper nanoparticles by molecular docking analysis. PLoS One 16(11):e0257959. *https://doi.org/10.1371/journal.pone.0257959*

Pahlsson, A.B (1989). Toxicity of heavy metals (Zn, Cu, Cd, Pb) to vascular plants. Water, Air, and Soil Pollution, 47:287-319. *https://doi.org/10.1007/bf00279329*

Pan B, Xing B (2012). Applications and implications of manufactured nanoparticles in soils: A review. European Journal of Soil Science 63(4):437-456. *https://doi.org/10.1111/j.1365-2389.2012.01475.x*

Payne GA (1998). Process of contamination by aflatoxin-producing fungi and their impacts on crops. In: Sinha KK, Bhatnagar D (Eds.). Mycotoxins in agricultural and food safety. Marcel Dekker, New York pp 1-18.

Pedregosa F, Varoquaux G, Gramfort A, Michel V, Thirion B, Grisel O, ... Duchesnay É (2011). Scikit-learn: Machine learning in Python. Journal of Machine Learning Research 12:2825-2830.

Reback J, McKinney W, Brockmendel J, Van Bossche J, Augspurger T, Cloud P, ... Seabold S (2021). Pandas-dev/pandas: Pandas 1.3.4. Zenodo. *https://doi.org/10.5281/zenodo.5574486*

Salvia AK, Nisha HAC, Raihan F, Tosnia T, Hossain MB (2023). Evaluation of the effect of fungicides, micronutrients, and botanicals on purple blotch complex of onion in Bangladesh. European Journal of Agriculture and Food Sciences 5(1): 97-102. *https://doi.org/10.24018/ejfood.2023.5.1.625*

Satour MM, Abd-El-Sattar MA, El-Wakil AA, El-Akkad EA, El-Ghareeb LA (1978). Fungi associated with stem and pod rot diseases of peanut in Egypt. In: Proceedings of the 10th Annual Meeting of the American Peanut Research and Education Association. Gainesville, FL pp. 45-52.

Singh A, Singh NB, Hussain I, Singh H, Yadav V, Singh SC (2016). Green synthesis of nano zinc oxide and evaluation of its impact on germination and metabolic activity of *Solanum lycopersicum.* Journal of Biotechnology 233:84-94. *https://doi.org/10.1016/j.jbiotec.2016.07.010*

Sirelkhatim A, Mahmud S, Azman S, Haida N, Mohamad K, Ann LC, Khadijah S, Bakhori M, Hasan H, Mohamad D (2015). Review on zinc oxide nanoparticles: Antibacterial activity and toxicity mechanism. Nano-Micro Letters 7(3):219-232. *https://doi.org/10.1007/s40820-015-0040-x*

Snell FD, Snell CI (1953). Colorimetric methods. Volume 3. D. Van Nostrand Company. Toronto, New York, and London pp 606.

Tarek AE, Amirah SA, Elkammar HF, Alothaim T, Ahmed NG, Abd Elmoneim D, ... Abou-Zeid MA (2024). Stimulating banana tree resistance to banana streak virus (BSV) disease by chitosan nanoparticles. European Journal of Plant Pathology 169:825-840. *https://doi.org/10.1007/s10658-024-02872-7*

Thimmaiah SK (1999). Standard methods of biochemical analysis. Kalyani Publishers, New Delhi p. 545.

Thomas W, Dutcher RA (1924). The colorimetric determination of carbohydrates in plants by the picric acid reduction method: I. The estimation of reducing sugars and sucrose. Journal of the American Chemical Society 46:1662-1669.

Tsewang T, Kapilab S, Kumara K, Verma V, Norbua A, Chaurasia OP, Acharya S (2024). Foliar application of zinc and boron improved physiological traits, productivity and shelf life of onion. Journal of Plant Nutrition 47(3):351-362. *https://doi.org/10.1080/01904167.2023.2276796*

USDA Department of Agriculture (2024). World agricultural production. Circular Series WAP 9-24. *https://apps.fas.usda.gov/psdonline/circulars/production.pdf*

Vijayreddy D, Dutta P, Puzari KR (2023). Nanotechnology in plant disease management. Research in Biotechnology 5(2):56-62. *https://doi.org/10.54083/ResBio/5.2.2023/56-62*

Walter WM, Purcell AE (1980). Effect of substrate levels on polyphenol oxidase activity and darkening in sweet potato cultivars. Journal of Agricultural and Food Chemistry 28:941-944. *https://doi.org/10.1021/jf60231a031*

Youssef SE, Mahmoud ME, Mounir AA (1999). Effect of chemical treatments on aflatoxin contamination and biochemical changes of peanut kernels caused by *A. parasiticus*. Egyptian Journal of Applied Sciences 14:40-52.

Zafar H, Alli A, Ali JS, Haq IU, Zia M (2016). Effect of ZnO nanoparticles on Brassica nigra seedlings and stem explants: Growth dynamics and antioxidative response. Frontiers in Plant Science 7:535. *https://doi.org/10.3389/fpls.2016.00535*

Zhang L, Wu X, Li J (2023). Dose-dependent responses of peanut to ZnO and MnO nanoparticles: Biochemical and physiological implications. Environmental Science & Technology 57(4):2894-2903. *https://doi.org/10.1021/acs.est.2c07284*

The journal offers free, immediate, and unrestricted access to peer-reviewed research and scholarly work. Users are allowed to read, download, copy, distribute, print, search, or link to the full texts of the articles, or use them for any other lawful purpose, without asking prior permission from the publisher or the author.

License - Articles published in ***Notulae Botanicae Horti Agrobotanici Cluj-Napoca*** are Open-Access, distributed under the terms and conditions of the Creative Commons Attribution (CC BY 4.0) License.

© Articles by the authors; Licensee UASVM and SHST, Cluj-Napoca, Romania. The journal allows the author(s) to hold the copyright/to retain publishing rights without restriction.

Notes:

- Material disclaimer: The authors are fully responsible for their work and they hold sole responsibility for the articles published in the journal.
- Maps and affiliations: The publisher stay neutral with regard to jurisdictional claims in published maps and institutional affiliations.
- Responsibilities: The editors, editorial board and publisher do not assume any responsibility for the article's contents and for the authors' views expressed in their contributions. The statements and opinions published represent the views of the authors or persons to whom they are credited. Publication of research information does not constitute a recommendation or endorsement of products involved.